Available online at www.sciencedirect.com
ScienceDirect
Bioorganic & Medicinal Chemistry 15 (2007) 2187–2197
Bioorganic & Medicinal Chemistry

Inhibition of FLT3 and PDGFR tyrosine kinase activity by bis(benzo[*b*]furan-2-yl)methanones☆

Siavosh Mahboobi,[a,*,†] Andrea Uecker,[b,†] Christophe Cénac,[a] Andreas Sellmer,[a] Emerich Eichhorn,[a] Sigurd Elz,[a] Frank-D. Böhmer[b,†] and Stefan Dove[a,*,†]

[a]*Institute of Pharmacy, Faculty of Chemistry and Pharmacy, University of Regensburg, D-93040 Regensburg, Germany*
[b]*Institute of Molecular Cell Biology, Jena University Hospital, D-07747 Jena, Germany*

Received 1 June 2006; revised 29 November 2006; accepted 8 December 2006
Available online 12 December 2006

Abstract—A series of bis(benzo[*b*]furan-2-yl)methanones was synthesized and tested for inhibition of FLT3 and PDGFR autophosphorylation. Mostly, C-5 substitution leads to PDGFR selectivity, which was strongest in the case of the 5,5′-dimethoxy derivative. The 5,5′-diamino and the 6,6′-dihydroxy compounds are more active at FLT3. At both kinases, the potency of the best inhibitors approaches IC_{50} values of ca. 0.5 μM. Molecular modeling studies suggest that the bisbenzofuranylmethanones are able to fit into the same binding site as their indolyl analogues which have been suggested to form a bidentate hydrogen bridge with the backbone in the hinge regions. The loss of one H bond by the NH–O exchange might be partially compensated by, for example, the weak interaction of one furanyl oxygen with FLT3 Cys-828.

1. Introduction

The platelet-derived growth factor receptor (PDGFR) and the Fms-like tyrosine kinase 3 (FLT3) have been implicated in a number of pathologies, especially in various cancers, and are therefore considered as drug targets (for review, see lit.[1,2]). Both are members of the class III receptor tyrosine kinase (RTK) family, which also includes the receptors for the stem cell factor (c-KIT), and for the colony stimulating factor 1 (CSF1R). The PDGF receptor is involved in wound healing and regulation of homeostasis of the connective tissue compartment. It is expressed on early stem cells, mast cells, myeloid cells, mesenchymal cells, and smooth muscle cells.[3] Overactivity/-expression of PDGFR has been implicated in malignancies as well as in different diseases involving excessive cell growth such as atherosclerosis and fibrosis. Therefore, a number of inhibitors targeting PDGFR are presently under development (for review see lit.[4]). The FLT3 receptor is crucial for the maintenance, proliferation, and differentiation processes in haematopoiesis. FLT3 is expressed by normal myeloid and lymphoid early progenitors as well as by leukemic cells.[5] Aberrant expression and/or mutation of FLT3 in acute myeloid leukemia (AML) and acute lymphoblastic leukemia (ALL) are the reasons for the great interest currently shown in the development of FLT3 inhibitors (for review, see lit.[6,7]).

Considering the structural similarities between FLT3 and PDGFR it is not too surprising that most of the small molecule inhibitors targeting one kinase are also more or less active against the other. Among these compounds are the quinoxalines AG1295,[8] AG1296,[8] and AGL2043,[8] the piperazinylquinazoline MLN518 (Tandutinib),[9] the indolocarbazole PKC412 (Midostaurin),[10] the indolinones SU5416 (Semaxanib)[11] and SU11248 (Sunitinib)[12] as well as the diarylurea BAY43-9006 (Sorafenib)[13] (Fig. 1). However, the indolocarbazole CEP701 (Lestaurtinib)[14] and the benzimidazolylquinolinone CHIR258[15] show highly significant selectivity for FLT3 versus PDGFR. On the other hand, the Abl/Bcr-Abl, c-KIT, and PDGFR inhibitor STI571 (Imatinib) is inactive against FLT3.[16,17]

We have previously identified bis(1*H*-indol-2-yl)methanone (**1a**) as a lead for the development of novel class

Keywords: Bisbenzofuranylmethanone; Receptor tyrosine kinase; FLT3; PDGFR; Bisindolylmethanone; Benzofuranylindolylmethanone.
☆ This paper is dedicated to Professor Wolfgang Wiegrebe on the occasion of his 75th birthday.
* Corresponding authors. Tel.: +49 0941 943 4824; fax: +49 0941 943 1737; e-mail addresses: siavosh.mahboobi@chemie.uni-regensburg.de; stefan.dove@chemie.uni-regensburg.de
† These authors contributed equally to this work.

0968-0896/$ - see front matter © 2007 Elsevier Ltd. All rights reserved.
doi:10.1016/j.bmc.2006.12.011

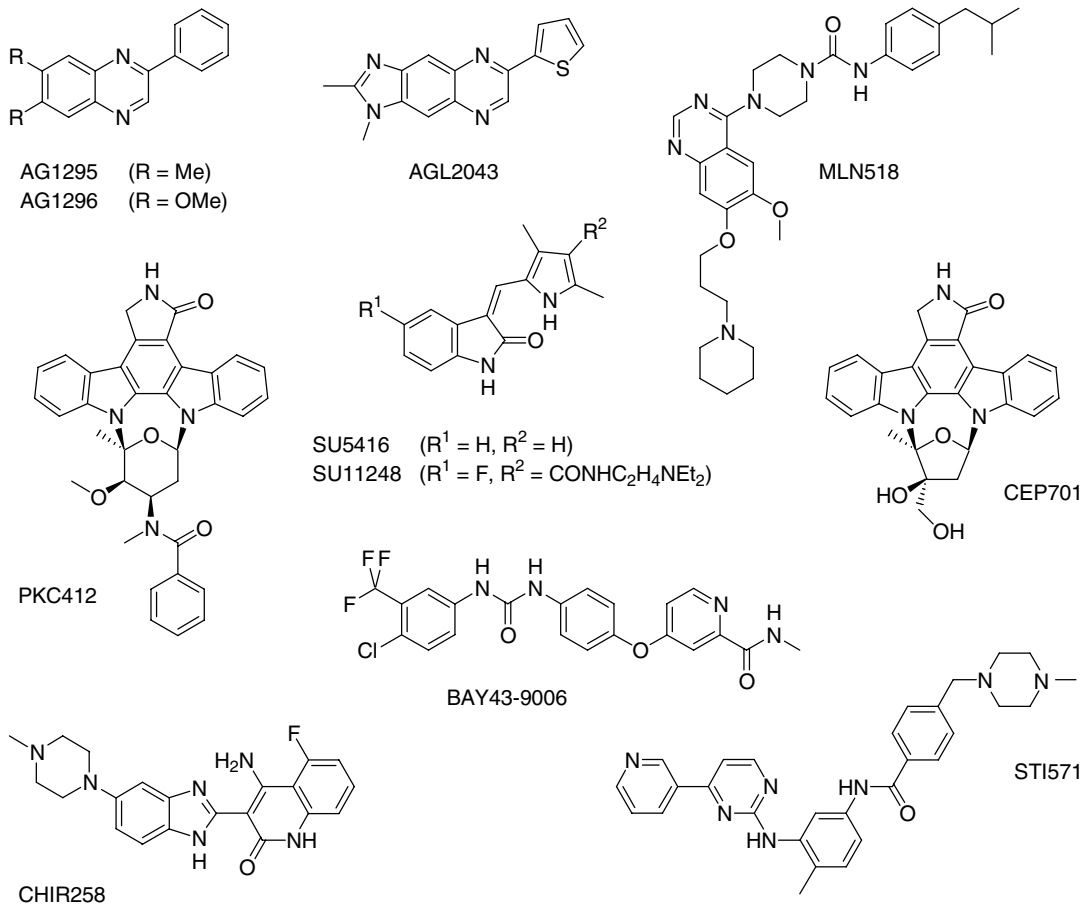

Figure 1. Small molecule inhibitors of FLT3 and/or PDGFR.

III RTK inhibitors[18] (cf. Fig. 2 and Table 1). PDGFR inhibition could be improved by hydroxy, methoxy, and carboxy substituents in 5-position of one indole moiety[18] (e.g., **1b**: IC_{50} = 0.3 μM and **1c**: IC_{50} = 0.2 μM). Further studies on disubstituted derivatives resulted in potent FLT3 inhibitors bearing at least one polar group at C-5, as for example, compound **1e**. The enhanced FLT3 inhibition is associated with a reasonable selectivity versus PDGFR[19] (cf. Table 1).

The bisindolylmethanones presumably dock into the ATP-binding pocket of PDGFR and FLT3 by forming a bidentate hydrogen bond with the backbone of PDGFR Cys-684 and FLT3 Cys-694, respectively, involving one indole NH and the CO of the methanone bridge.[18,19] Symmetrical bis(benzo[*b*]furan-2-yl)methanones are already known as Tilorone analogues[20] and antiviral agents,[21–24] as possible aldose reductase inhibitors, and platelet aggregation inhibitors,[23] or as charge-generating compounds in the photosensitive layer of photoreceptors.[25] As described here, PDGFR and FLT3 can also be inhibited by bisbenzofuranylmethanones. Most of these compounds are less potent than their corresponding bisindolylmethanone homologues, however, the unsubstituted leads are nearly equiactive. Therefore, one of the suggested hydrogen bonds which is disabled by the NH–O exchange should be replaced by another interaction. This may be an H bond of one of the oxygens, since the corresponding bisbenzothiophenyl analogue is inactive.[18] The resulting specific binding mode of the bis(benzo[*b*]furan-2-yl)methanones alters the structure–activity and structure–selectivity relationships observed in the bis(1*H*-indol-2-yl)methanone series.

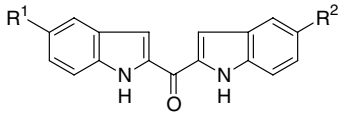

	R^1	R^2	
	H	H	**1a**
	OMe	H	**1b**
	OH	H	**1c**
	OMe	OMe	**1d**
	OH	OH	**1e**

Figure 2. Bis(1*H*-indol-2-yl)methanone (**1a**) and selected derivatives with tyrosine kinase inhibition properties.

2. Chemistry

The first stage of our study consisted in the synthesis of the oxygen isostere of bisindolylmethanone **1a**, and a series of methoxy-disubstituted bisbenzofuranylmethanones. Chemical modification was then performed in positions 5, 6, and 7. Salicylaldehyde as well as its 6-, 5-, 4-, 3-methoxy and 5-nitro derivatives were condensed with 1,3-dihaloacetone in order to obtain the corresponding symmetric bisbenzofuranylmethanones **2**–**6**

Table 1. Inhibition of PDGFR and FLT3 tyrosine kinases by bis(benzo[*b*]furan-2-yl)methanones and related compounds

Compound	X	Position	R	PDGFR[a] IC_{50} (μM)	FLT3[b] IC_{50} (μM)
			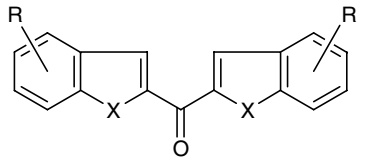		
1a[c,d]	NH	—	H	1	4.6
1d[c]	NH	5	OCH_3	10–30	>10
1e[d]	NH	5	OH	0.3	0.04
2	O	—	H	1.2	3.5
3	O	4	OCH_3	>30	>30
4	O	5	OCH_3	1.0	>30
5	O	6	OCH_3	>30	>30
6	O	7	OCH_3	>30	>30
7	O	5	OH	0.6	3.6
8	O	6	OH	9.7	1.8
9	O	7	OH	20–30	>30
10	O	5	$OCOCH_3$	0.7	1.7
12	O	5	NH_2	1.2	0.6
			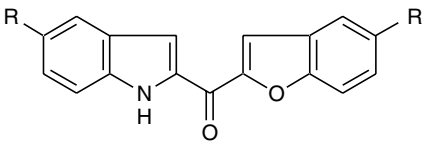		
23			H	1.07	0.40
25			OH	0.20	0.27
			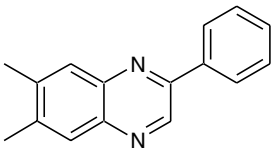		
AG1295				5.4	1.1

[a] Assayed with endogenous PDGFR in Swiss 3T3 fibroblasts.
[b] Assayed with endogenous FLT3 in EOL-1 cells.
[c] Previously published results on PDGFR inhibition.[18]
[d] Previously published results on PDGFR and FLT 3 inhibition.[19]

and **11** in one step according to Royer et al.[20] (see Scheme 1). The 5-, 6-, and 7-OMe-disubstituted bis(benzo[*b*]furan-2-yl)methanones were then demethylated with pyridine hydrochloride under microwave irradiation in order to obtain their respective dihydroxylated derivatives **7**–**9**. Subsequent acetylation of the 5,5′-dihydroxy derivative led to the diester **10**. Hydrogenolytic palladium-catalyzed reduction of the dinitro-functionalized compound **11** led to the diamine **12**.

In addition, we prepared hybrid benzofuranylindolylmethanones to validate the proposed SARs and binding mode (derivatives **23** and **25**). The synthetic route[26] is shown in Scheme 2: metalation of the suitable N-protected indoles (**19** and **20**) by use of *n*-butyllithium in THF solution, followed by coupling with the respective benzo[*b*]furan-2-carbonyl chlorides, yielded the (benzo[*b*]-furan-2-yl)-(1-phenylsulfonyl-1*H*-indol-2-yl)methanones **21** and **22**, which were deprotected by NaOH to yield the desired hybrid derivatives **23** and **24**. In case of **24** hydrogenolytic cleavage of both benzyloxy groups[18,19] was subsequently performed to give the 5,5′-diOH compound **25** in excellent yield.

The respective benzofurancarbonyl chlorides used for the synthesis (**17**[27] and **18**) were prepared by chlorination of their corresponding carboxylic acids (Scheme 2). The 5-benzyloxybenzo[*b*]furan-2-carboxylic acid **16**[28] hereby was accessible in four steps (see Scheme 3) from 5-hydroxy-2-methoxybenzaldehyde as follows: ring closure with bromoacetic acid ethyl ester led to the 5-methoxybenzo[*b*]furan-2-carboxylic acid ethyl ester **13**,[29] subsequent demethylation with boron tribromide, followed by benzylation of the phenol intermediate **14**,[29] led to **15**.[30] Alkaline cleavage of the ethyl ester group afforded the desired compound **16** in the following.

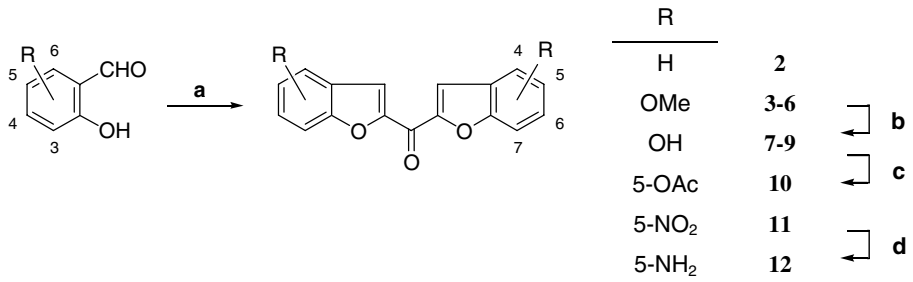

Scheme 1. Synthesis of bisbenzofuranylmethanones. Reagents and conditions: (a) $(ClCH_2)_2CO$ or $(BrCH_2)_2CO$, K_2CO_3, EtCOMe, Δ; (b) pyridinium chloride, MW; (c) AcCl, DMAP, AcOMe, pyridine; (d) HCO_2NH_4, Pd/C, *i*PrOH, Δ.

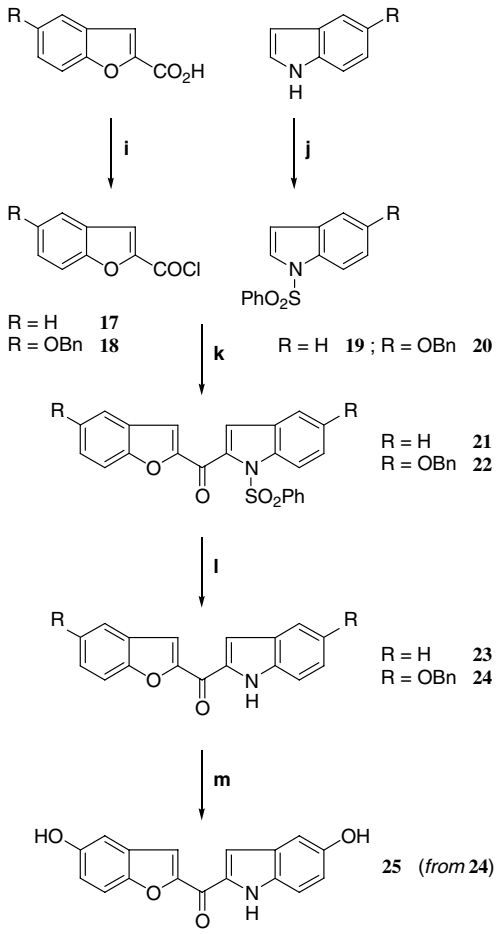

Scheme 2. Synthesis of benzofuranylindolylmethanones. Reagents and conditions: (i) $SOCl_2$ (1.04 equiv), Pyridine (1.1 equiv), DCM; (j) 1—NaH, THF; 2—$PhSO_2Cl$, 0 °C; (k) *n*BuLi, THF, −78 °C; (l) 1—NaOH, MeOH, THF, Δ; 2—HCl; (m) HCO_2NH_4, Pd/C, MeOH, Δ.

3. Results and discussion

The biological activities of the bis(benzo[*b*]furan-2-yl)methanones are summarized in Table 1, with exception of the 5,5′-dinitro derivative **11** whose solubility was too low to proceed with the usual testing procedures. The (benzo[*b*]furan-2-yl)-(1*H*-indol-2-yl)methanone (**23**) and its 5,5′-dihydroxy derivative **25** were also tested for RTK inhibition in order to probe the binding mode hypothesis. The quinoxaline AG1295[8] was used as a standard.

The unsubstituted bisbenzofuranylmethanone **2** inhibited both kinases with similar potency and with the same selectivity for PDGFR as the bisindolylmethanone **1a**. The PDGFR inhibition of the 5,5′-diOMe-substituted bisbenzofuranylmethanone derivative **4** is in the same range (IC_{50} = 1.0 μM) and associated with significant selectivity versus FLT3 (IC_{50} > 30 μM). In contrast, its bisindolyl analogue **1d** is inactive at both kinases. The 4,4′-, 6,6′-, or 7,7′-diOMe-substituted bisbenzofuranylmethanones **3**, **5** and **6** did not inhibit PDGFR and FLT3 in concentrations up to 30 μM. As in the case of the bisindolylmethanones, 5- or 6-dihydroxy is more favorable than 5- or 6-dimethoxy substitution. The 6,6′-diOH derivative **8** is slightly FLT3 selective, attributed to reduced PDGFR inhibition (IC_{50} = 9.7 μM), and a twofold higher potency against FLT3 compared to the unsubstituted compound. In contrast the 5,5′-diOH positional isomer **7** is sixfold more potent at PDGFR than at FLT3. These results are opposed to the data of the corresponding bisindolylmethanones where 5,5′-diOH substitution leads to significant FLT3 selectivity (cf. **1e**), whereas polar 6-substituents mostly reduce FLT3 inhibition.[19] The 7,7′-diOH derivative **9** was inactive at FLT3 and PDGFR. Surprisingly acetylation of the 5,5′-diOH derivative did not significantly

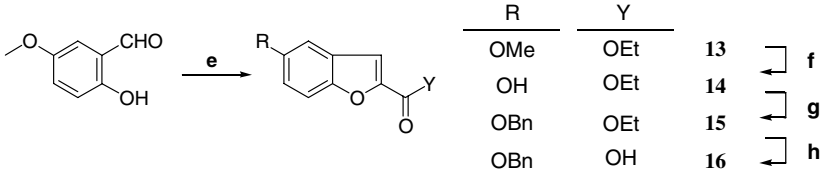

Scheme 3. Synthesis of the 5-benzyloxybenzo[*b*]furan-2-carboxylic acid **16**. Reagents and conditions: (e) $BrCH_2CO_2Et$, K_2CO_3, DMF, Δ; (f) BBr_3 (2.5 equiv), DCM, 0 °C; (g) BnBr (1.2 equiv), K_2CO_3 (4 equiv), Me_2CO, Δ; (h) KOH [2 N], H_2O, MeOH, THF.

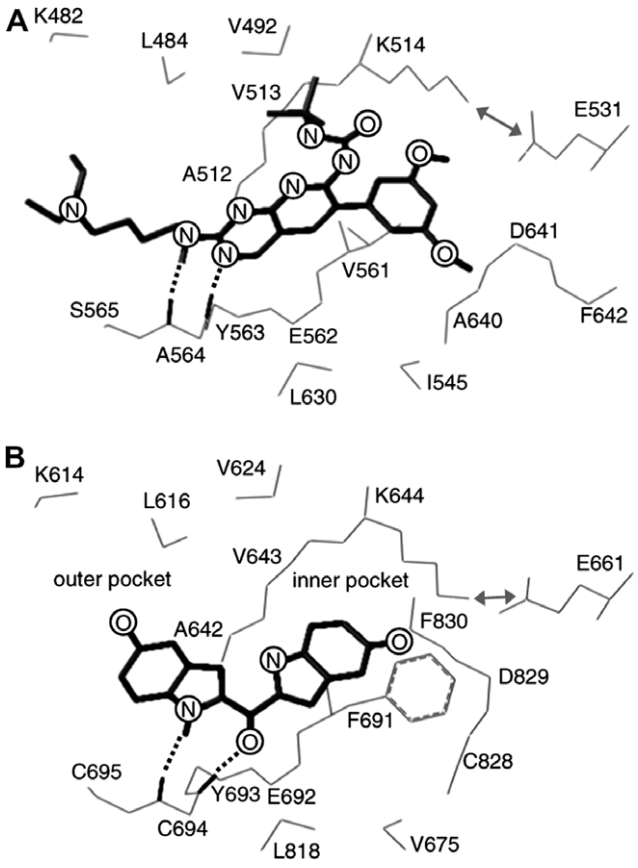

Figure 3. Comparison of (A) the binding mode of PD-173074 at the FGFR-1 with (B) the suggested binding mode of the bisindolylmethanone **1e** at FLT3. The crystal structure of the FGFR-1 PD-173074 complex (PDB 2fgi) was aligned with the minimized FLT3 structure (from PDB 1rjb) containing **1e**. For the superposition, the backbone atoms of the FLT3 residues lying within 4 Å around **1e** were used as template for the corresponding FGFR-1 amino acids (rms without the strongly deviating Phe-830/Phe-642 in the DFG motif: 0.96 Å). FLT3 Phe-691 (FGFR-1 Val-561) is the only residue which differs from PDGFR (Thr-681). Arrows, salt bridge between Glu and Lys; dotted lines, bidentate hydrogen bonds.

change activity against both kinases (compd **10**). 5,5′-DiNH_2 substitution (compd **12**) improved FLT3 inhibition, and maintained PDGFR inhibition compared to the unsubstituted and the 5,5′-diOH analogues.

The hybrid benzofuranylindolylmethanone **23** was significantly more potent as FLT3 and equiactive as PDGFR inhibitor compared to its 'pure' indolyl and benzofuranyl analogues (**1a** and **2**). 5,5′-Dihydroxy substitution (compd **25**) slightly improves activity at both kinases, but does neither lead to FLT3 nor to PDGFR selectivity like in the case of the corresponding bisindolylmethanone **1e** and bisbenzofuranylmethanone **7**, respectively.

More detailed discussions of the SAR must consider the probable binding mode and the symmetry of the bis(benzo[*b*]furan-2-yl)methanone scaffold. As suggested from a homology model of the PDGFR,[18] from the recent crystal structure (PDB 1rjb) of FLT3,[31] and from SAR of bis(1*H*-indol-2-yl)methanones,[18,19] the bisindolylmethanone derivatives may bind to the ATP site in a mode resembling the interaction of PD-173074 in a crystallized complex with the FGFR-1[32] (see Fig. 3). The key interactions are two hydrogen bonds of an indole NH and the methanone oxygen with the CO and the NH moiety, respectively, of the backbone of FLT3 Cys-694 (PDGFR Cys-684). Bisindolylmethane derivatives are inactive.[19] The bidentate hydrogen bond donor–acceptor system results in one indole ring pointing inwards and the other pointing outwards, and thereby enables the definition of an inner and an outer binding pocket. The outer indole is open for substitution in positions 5 and 6 even with larger polar, for example, piperidinoethoxy or quinolylcarboxy groups.[18,19] The substituents are surrounded by short chains of the β1 strand and of the hinge region, and protrude into the solvent.

The question arises whether the bis(benzo[*b*]furan-2-yl)methanones may bind to the ATP site of FLT3 and PDGFR similarly as the bisindolylmethanones even though one of the H bonds, namely the one disabled by the NH–O exchange, cannot be formed. Since the unsubstituted leads **1a** and **2** are nearly equiactive, this hydrogen bond should be replaced by another interaction, possibly an H bond of one of the oxygens, since the corresponding bisbenzothiophenyl analogue is inactive.[18] To check this hypothesis, the 5,5′-diOH derivative **7** was docked into the putative bisindolylmethanone binding site of the FLT3 crystal structure 1rjb (see Fig. 4).

Generally each benzofuranyl moiety may be synperiplanar (*sp*, *cis*) or antiperiplanar (*ap*, *trans*) with the carbonyl function if the OC–CO torsion angles are taken as reference. AMPAC 8.15 calculations of compound **7** with the COSMO water solvation model result in the lowest energy for a *ap*/*sp* planar conformation. However, the *sp*/*sp* and *ap*/*ap* conformers are only 0.12 and 0.72 kcal/mol, respectively, higher in energy. The rotational barrier around one of the OC–CO bonds amounts to 2.7 kcal/mol. Also in the unsolvated state, the *ap*/*sp* conformer represents the global minimum. In conclusion, each binding conformation with nearly coplanarity of both benzofuranyl moieties is energetically possible, but an *ap*/*sp* geometry is preferred.

The docking mode in Figure 4 shows the outer benzofuranyl moiety in *ap* orientation since the furanyl oxygen should not point to the backbone O atom of Cys-694. Then, however, the inner benzofurane ring may be *sp* with the carbonyl function. This conformation may enable the inner furanyl oxygen to form a weak H bond with the SH group of Cys-828 preceding the DFG motif (O···HS distance 2.25 Å) and the lipophilic edge of the benzofurane moiety to fit to a hydrophobic pocket (Val-624, Ala-642).

Compound **7** fits to a bank of four residues, Phe-691 to Cys-694, belonging to β5 and the hinge region. Within 3 Å around the ligand, Phe-691 is the only mutated amino acid compared to the PDGFR (Thr-681) and, therefore, the primary candidate for explaining selectivity. Lys-644 (β3) and Glu-661 (αC), forming a salt bridge

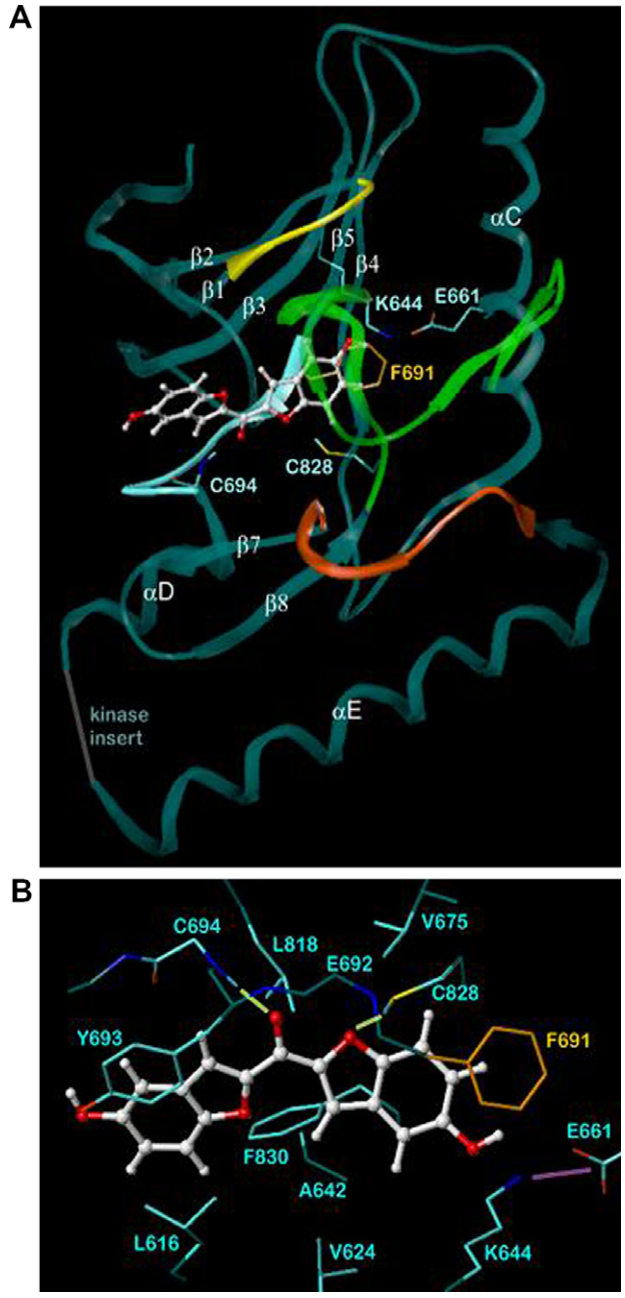

Figure 4. Suggested binding mode of the bisbenzofuranylmethanone derivative **7** at FLT3 demonstrated by a minimized complex with the FLT3 crystal structure 1rjb.[31] (A) Overview of the model with compd **7** and with representation of some important amino acids. Specific regions are highlighted on the ribbon/tube backbone: light cyan—inhibitor binding site consisting of parts of β5 and the hinge region, yellow—nucleotide binding loop, red orange—catalytic loop, green—activation loop. Other important secondary structure elements are indicated at the backbone. The view is from the C-terminus and corresponds approximately to the views in Fig. 3. The C-terminal part after the activation loop is not displayed. (B) Detailed view of the binding site of compd **7** with all amino acids lying within a sphere of 3.5 Å around the ligand. Backbone atoms are dark, side chains light cyan. C atoms orange—Phe-691. Yellow lines—hydrogen bonds of Cys-694 and Cys-828 with the ligand. Purple line—salt bridge.

as in other tyrosine kinases, are close to the 5- and 6- positions of the inner benzofuranyl moiety whose binding site is completed by the side chains of Ala-642 (β3) from the top and of Val-624 (β2), Leu-818 (β7), and Phe-830 (DFG-motif) from the bottom. The outer benzofuranyl moiety interacts with the N-terminal domain residues Leu-616 (β1) and Tyr-693 (hinge) as well as with Phe-830.

The suggested *ap*/*sp* binding mode of the bisbenzofuranylmethanones is directly opposed to the proposed *sp*/*ap* mode of the bisindolyl compounds (compare Fig. 3B and Fig. 4B) which best explains the structure–selectivity relationships in this series.[19] The different conformations formally result in an alignment of the indolyl-5 with the benzofuranyl-6 position and vice versa. In some respects this corresponds to the opposite impact of 5- and 6-hydroxy groups on PDGFR and FLT3 inhibition: 5-OH indolyl and 6-OH benzofuranyl structures tend to FLT3, 5-OH benzofuranyl and many 6-substituted indolyl moieties[19] to PDGFR selectivity. The preference of the 5-hydroxy (**7**), 5-methoxy (**4**), and 5-acetoxy (**10**) benzofuranyl moieties for PDGFR may be explained by electrostatic interaction of the O atoms with the OH group of Thr-681. On the other hand, the inactivity of compounds **4** and **5** at FLT3 should be based on repulsion between the methoxy substituents and Phe-691.

Figure 4 shows that the outer benzofuranyl moiety protrudes into the solvent. Obviously, the 5- and 6-positions are free and remain solvated in the bound state. Substituents in 4- and 7-positions are sterically hindered by β1 and the hinge region like in the case of the bisindolylmethanones,[19] leading to inactivity of compounds **3**, **6** and **9** at both kinases.

The higher FLT3 inhibition of the hybrids (compare **23** to **1a** and **2**, **25** to **7**) indicates an *sp*/*sp* binding mode with formation of the bidentate H bond like in the case of the bisindolylmethanones. The inner 5′-OH-benzofuranyl moiety of compound **25** does probably not similarly fit to the binding site like the 5′-OH-indolyl moiety of **1e** suggested to bind in *sp*/*ap* mode, since **1e** is by a factor of seven more active than the hybrid **25**. As mentioned above, this *ap* conformation is unfavorable for an inner benzofuranyl moiety (no H bond with the SH of Cys-828). In the case of PDGFR inhibition, the hybrids **23** and **25** do not improve the activity of the "pure" analogues. This is not surprising since the potency of the latter is very similar, too (cf. **1a** with **2**, **1e** with **7**). Thus, no additional information about the PDGFR binding mode can be obtained from the present data of the hybrids.

The model depicted in Figure 4 does not explain all of the structure–activity and structure–selectivity relationships. Detailed topological differences of the binding sites remain unsolved due to the lack of a PDGFR crystal structure. The relatively high activity of the 5,5′-diacetoxy derivative **10** at FLT3 is somewhat surprising compared to its inactive 5,5′-dimethoxy analogue **4**. However, the binding site offers some degrees of freedom in the direction of the 5- and 6-positions of the inner benzofuranyl moiety, as shown by the high inhibitory potency of STI-571 at the FLT3 Phe-691-Thr

mutant.[17] Also the lower FLT3 activity of the 5,5′-dihydroxy derivative **7** versus the 5,5′-diamino analogue **12** cannot be explained by the model since both compounds should be able to interact with Glu-661 (distance ca. 2.8 Å). The SAR as well as the modeling of the new series do not provide further reasons for the extraordinary high and selective inhibition of FLT3 by the 5,5′-diOH bisindolylmethanone **1e**. Generally the possibility cannot be ruled out that in some cases the measured IC_{50} values are based on a mixture of different bound conformations and/or even different binding modes at both kinases.

4. Conclusions

Bis(benzo[*b*]furan-2-yl)methanones are FLT3 and PDGFR tyrosine kinase inhibitors exhibiting IC_{50} values in the low micromolar range. The unsubstituted compound **2** is as active as the corresponding bis(1*H*-indol-2-yl)methanone **1a**. In contrast to the former bisindolylmethanone series, the potency could not be strongly improved by introduction of substituents. Most effective was a 5,5′-diamino substitution (compd **12** with sixfold lower IC_{50} value than **2** against FLT3). A high degree of selectivity for PDGFR versus FLT3 was observed for the 5,5′-dimethoxy-substituted derivative **4**. At both kinases, the bisbenzofuranyl- and their bisindolylmethanone analogues are suggested to fit to the same binding site, but with different conformations resulting from the formation of individual hydrogen bonds and accounting for the opposite impact of 5- and 6-hydroxy groups on PDGFR and FLT3 inhibition: 5,5′-diOH bisindolyl- and 6,6′-diOH bisbenzofuranylmethanones tend to FLT3, 5,5′-diOH bisbenzofuranyl derivatives to PDGFR selectivity. Further modifications of the structures, in particular the investigation of unsymmetric substitution patterns, will possibly lead to more potent inhibitors with higher selectivity for one of both kinases.

5. Experimental protocols

5.1. Chemical procedures

5.1.1. General aspects. The methyl ethers of compounds **4**, **5**, and **6** were cleaved under microwave irradiation using a CEM Discover-focused microwave synthesis system. Melting points were determined with a BÜCHI Melting Point B-545 device. IR spectra (pure solid if no contrary indication is given) were measured with a BRUKER Tensor 27. ^{1}H NMR spectra were recorded with a BRUKER Avance 300 (300 MHz) at 300 K, using solvent peak as internal standard. MS spectra were measured with a FINNIGAN MAT 95.

5.1.2. Syntheses

5.1.2.1. Procedure a—Synthesis of bis(benzo[*b*]furan-2-yl)methanones from 2-hydroxybenzaldehyde derivatives. Potassium carbonate (17 g, 1 equiv) was added to a hot butanone solution (250 mL) of salicylaldehyde (15 g, 122.8 mmol) and 1,3-dihaloacetone (7.8 g, 0.5 equiv), before refluxing the mixture for 4 h. The suspension was filtered, the resulting solution was washed with water and evaporated. The obtained residue was subjected to column chromatography (SiO_2, ethyl acetate) and then recrystallized.

5.1.2.2. Bis(benzo[*b*]furan-2-yl)methanone (2). Preparation from salicylaldehyde (Lancaster) as described above, using 1,3-dichloropropan-2-one. Yield: 9.62 g (60%) of colorless crystals. Mp 156 °C (from dichloromethane), lit.[33] 155–157 °C. ^{1}H NMR (DMSO-d_6): δ (ppm) = 7.40 (dd, 2H, J = 7.7 Hz, 7.1 Hz), 7.59 (dd, 2H, J = 8.2 Hz, 7.1 Hz), 7.79 (d, 2H, J = 8.2 Hz), 7.90 (d, 2H, J = 7.7 Hz), 8.22 (s, 2H).

5.1.2.3. Bis(4-methoxybenzo[*b*]furan-2-yl)methanone (3). Preparation from 2-hydroxy-6-methoxybenzaldehyde (Lancaster) as described above, using 1,3-dibromopropan-2-one. Yield: 1.59 g (15%) of light yellow crystals. Mp 195–196 °C (from acetone), lit.[22] 181–183 °C. ^{1}H NMR (DMSO-d_6): δ (ppm) = 3.97 (s, 6H), 6.92 (d, 2H, J = 8.0 Hz), 7.40 (d, 2H, J = 8.5 Hz), 7.54 (dd, 2H, J = 8.5 Hz, 8.0 Hz), 8.10 (s, 2H).

5.1.2.4. Bis(5-methoxybenzo[*b*]furan-2-yl)methanone (4). Preparation from 2-hydroxy-5-methoxybenzaldehyde (Acros and Lancaster) as described above, using 1,3-dichloropropan-2-one. Yield: 8.70 g (50%) of light yellow crystals. Mp 175 °C (from dichloromethane), lit.[22] 173–174 °C, lit.[20] 176 °C. ^{1}H NMR (DMSO-d_6): δ (ppm) = 3.82 (s, 6H), 7.20 (dd, 2H, J = 9.0 Hz, 2.5 Hz), 7.35 (d, 2H, J = 2.5 Hz), 7.71 (d, 2H, J = 9.0 Hz), 8.12 (s, 2H).

5.1.2.5. Bis(6-methoxybenzo[*b*]furan-2-yl)methanone (5). Preparation from 2-hydroxy-4-methoxybenzaldehyde (Acros) as described above, using 1,3-dichloropropan-2-one. Yield: 6.07 g (29%) of yellow crystals. Mp 203–204 °C (from toluene), lit.[22] 191–193 °C, lit.[20] 200 °C. ^{1}H NMR (DMSO-d_6): δ (ppm) = 3.87 (s, 6H), 7.04 (d, 2H, J = 8.8 Hz), 7.40 (s, 2H), 7.76 (d, 2H, J = 8.8 Hz), 8.13 (s, 2H).

5.1.2.6. Bis(7-methoxybenzo[*b*]furan-2-yl)methanone (6). Preparation from 2-hydroxy-3-methoxybenzaldehyde (Aldrich) as described above, using 1,3-dichloropropan-2-one. Yield: 10.31 g (64%) of colorless crystals. Mp 146–147 °C (from methanol), lit.[22] 143–144 °C. ^{1}H NMR (DMSO-d_6): δ (ppm) = 4.00 (s, 6H), 7.18 (d, 2H, J = 8.0 Hz), 7.32 (dd, 2H, J = 8.0 Hz, 8.0 Hz), 7.45 (d, 2H, J = 8.0 Hz), 8.13 (s, 2H).

5.1.2.7. Bis(5-nitrobenzo[*b*]furan-yl)methanone[25] (11). Preparation from 2-hydroxy-5-nitrobenzaldehyde (Lancaster) as described above, using 1,3-dichloropropan-2-one. Yield: 1.4 g (13%) of colorless crystals. Mp 294 °C (washed with acetone). ^{1}H NMR (DMSO-d_6): δ (ppm) = 8.08 (d, 2H, J = 9.1 Hz), 8.45 (s, 2H), 8.47 (dd, 2H, J = 9.1 Hz, 2.5 Hz), 8.89 (d, 2H, J = 2.5 Hz).

5.1.2.8. Procedure b—Demethylation of compounds 4–6 leading to the corresponding bisbenzofuranylmethanone dihydroxylated derivatives. A mixture of a dimethoxylated bisbenzofuranylmethanone derivative (1.53 g,

4.75 mmol) and pyridinium chloride (8.3 g, 15 equiv) was heated to 160 °C, while stirring, in a focused microwave apparatus (300 W, 5 min). The hot melt was hydrolyzed to leave a solid residue which was collected on filter, washed with water, dried, and subjected to column chromatography (SiO_2, ethyl acetate) before recrystallization.

5.1.2.9. Bis(5-hydroxybenzo[*b*]furan-2-yl)methanone (7). Preparation from bis(5-methoxybenzo[*b*]furan-2-yl)methanone **4** as described above. Yield: 1.90 g (72%) of yellow crystals. Mp dec 280 °C (from EtOH/toluene), lit.[22] dec 277–278 °C, lit.[20] dec 287 °C. ^{1}H NMR (DMSO-d_6): δ (ppm) = 7.04 (dd, 2H, J = 8.8 Hz, 2.5 Hz), 7.15 (d, 2H, J = 2.5 Hz), 7.60 (d, 2H, J = 8.8 Hz), 8.05 (s, 2H), 9.58 (s, 2H).

5.1.2.10. Bis(6-hydroxybenzo[*b*]furan-2-yl)methanone (8). Preparation from bis(6-methoxybenzo[*b*]furan-2-yl)methanone **5** as described above. Yield: 1.77 g (67%) of yellow crystals. Mp dec 263–264 °C (from acetone), lit.[22] dec 256–258 °C, lit.[20] dec 270 °C. ^{1}H NMR (DMSO-d_6): δ (ppm) = 6.90 (dd, 2H, J = 8.5 Hz, 2.0 Hz), 7.06 (m, 2H), 7.67 (d, 2H, J = 8.5 Hz), 8.06 (m, 2H), 10.24 (s, 2H).

5.1.2.11. Bis(7-hydroxybenzo[*b*]furan-2-yl)methanone (9). Preparation from bis(7-methoxybenzo[*b*]furan-2-yl)methanone **6** as described above. Yield: 1.08 g (77%) of yellow crystals. Mp dec 268–269 °C (from dichloromethane), lit.[22] dec 268–269 °C. ^{1}H NMR (DMSO-d_6): δ (ppm) = 7.00 (d, 2H, J = 7.2 Hz), 7.20 (dd, 2H, J = 7.2 Hz, 7.2 Hz), 7.32 (d, 2H, 7.2 Hz), 8.21 (s, 2H), 10,46 (s, 2H).

5.1.2.12. Procedure c—Esterification of bis(5-hydroxybenzo[*b*]furan-2-yl)methanone (7). Acetyl chloride (2.2 mL, 6 equiv) was added to a solution of bis(5-hydroxybenzo[*b*]furan-2-yl)methanone (1.54 g, 5.2 mmol) and a catalytic quantity of DMAP in methyl acetate (20 mL) and pyridine (5 mL). After a 12-h stirring time, the solution was poured into an ice/water mixture (25 mL). Extraction with ethyl acetate, drying of the combined organic layers over magnesium sulfate, and distillation of the solvent left the crude product witch was recrystallized from dichloromethane.

5.1.2.13. Bis(5-acetoxybenzo[*b*]furan-2-yl)methanone (10). Yield: 1.44 g (73%) of colorless crystals. Mp 209.5–210.5 °C (from dichloromethane), lit.[24] 203–204 °C. ^{1}H NMR (DMSO-d_6): δ (ppm) = 2.31 (s, 6H), 7.37 (dd, 2H, J = 9.1 Hz, J = 2.5 Hz), 7.67 (d, 2H, J = 2.5 Hz), 7.85 (d, 2H, J = 9.1 Hz), 8.23–8.24 (m, 2H).

5.1.2.14. Procedure d—Preparation of derivate 12 by reduction of the 5,5′-dinitro compound 11. 1.6 g (9 equiv) of ammonium formate and 0.1 g of activated Pd/C (10%) were added to a hot suspension of **11** (900 mg) in propan-2-ol (250 mL) and the mixture was gently refluxed for 48 h. The solution was cooled down to rt, the catalyst filtered off, and the solvent evaporated. Ethyl acetate and water were added, the organic layer was washed with water and dried (Na_2SO_4). Treatment of the residue with a little diethyl ether results in crystallization of the compound, which was washed with additional ether.

5.1.2.15. Bis(5-aminobenzo[*b*]furan-2-yl)methanone[25] (12). Yield: 0.54 g (70%) of red-orange crystals. Mp dec 189 °C (from diethyl ether). ^{1}H NMR (DMSO-d_6): δ (ppm) = 5.28 (s, 4H), 6.88–6.92 (m, 4H), 7.46 (dd, 2H, J = 9.6 Hz, J = 0.8 Hz), 7.93 (d, 2H, J = 0.8 Hz).

5.1.2.16. Procedure e—Preparation of 5-methoxybenzo[*b*]furan-2-carboxylic acid ethyl ester (13). The synthesis was performed according to lit.[29] Yield: 9.2 g (61%) of a colorless solid. ^{1}H NMR ($CDCl_3$): δ (ppm) = 1.43 (t, 3H, J = 7.1 Hz), 3.85 (s, 3H), 4.44 (qu, 2H, J = 7.1 Hz), 7.05–7.08 (m, 2H), 7.47–7.50 (m, 2H).

5.1.2.17. Procedure f—Demethylation of compound 13. The desired compound was prepared by a modification of lit.[29] as follows: 5-methoxybenzo[*b*]furan-2-carboxylic acid ethyl ester (9.0 g, 40.9 mmol) was dissolved in dichloromethane (300 mL), boron tribromide (2.5 equiv) was added at 0 °C. After a 1 h stirring period at 0 °C, the mixture was poured into saturated brine (200 mL), the organic layer separated, dried (Na_2SO_4), the solvent removed under reduced pressure, and the title compound purified by column chromatography (SiO_2, CH_2Cl_2).

5.1.2.18. 5-Hydroxybenzo[*b*]furan-2-carboxylic acid ethyl ester (14). Yield: 5.95 g (71%) of a colorless solid. ^{1}H NMR ($CDCl_3$): δ (ppm) = 1.43 (t, 3H, J = 7.1 Hz), 4.44 (q, 2H, J = 7.1 Hz), 5.57 (s, 1H, exchangeable), 7.01 (dd, 1H, J = 9.1 Hz, 2.5 Hz), 7.08 (d, 1H, J = 2.5 Hz), 7.42–7.44 (m, 2H).

5.1.2.19. Procedure g—Benzylation of compound 14. 5-Hydroxybenzo[*b*]furan-2-carboxylic acid ethyl ester (6.0 g, 20.09 mmol) was dissolved in acetone (120 mL), benzyl bromide (1.2 equiv) and potassium carbonate (4 equiv) were added, and the mixture stirred at reflux for 3 h. The solvent was removed under reduced pressure, the mixture extracted with dichloromethane, and the title compound purified by column chromatography (SiO_2, CH_2Cl_2).

5.1.2.20. 5-Benzyloxybenzo[*b*]furan-2-carboxylic acid ethyl ester[30] (15). Yield: 7.30 g (85%) of a colorless solid. Mp 83.9–85.3 °C. IR (KBr): ν (cm^{-1}) = 1609. ^{1}H NMR (DMSO-d_6): δ (ppm) = 1.32 (t, 3H, J = 7.1 Hz), 4.34 (q, 2H,, J = 7.1 Hz), 5.13 (s, 2H), 7.19 (dd, 1H, J = 7.1 Hz, 2.5 Hz), 7.32–7.65 (m, 8H).

5.1.2.21. Procedure h—Deesterification of compound 15. A mixture of 5-benzyloxybenzo[*b*]furan-2-carboxylic acid ethyl ester (7.00 g, 23.6 mmol), THF, EtOH and 2 N KOH (150 mL, 1:1:1) was stirred at room temperature for 4 h. The organic solvents were removed under reduced pressure, the residue dissolved in water (100 mL), acidified with concd HCl, extracted with ethyl acetate (3× 100 mL), and the combined organic layers dried (Na_2SO_4). Most of the solvent was removed under reduced pressure and the title compound crystallized by addition of pentane.

5.1.2.22. 5-Benzyloxybenzo[*b*]furan-2-carboxylic acid[28] (16). Yield: 7.30 g (71%) of colorless crystals. Mp 182.6–184.3 °C. IR (KBr): ν (cm^{-1}) = 2959, 1726. ^1H NMR (DMSO-d_6): δ (ppm) = 5.13 (s, 2H), 7.13 (dd, 1H, J = 9.1 Hz, 2.7 Hz), 7.31–7.51 (m, 7H), 7.58 (d, 1H, J = 9.1 Hz), 13.60 (s, br s 1H, exchangeable).

5.1.2.23. Procedure i—Preparation of benzo[*b*]furan-2-carbonyl chlorides. To a stirred dichloromethane solution (20 mL, dry) of the respective benzo[*b*]furan-2-carboxylic acid (15.42 mmol), pyridine (1.39 mL, 17 mmol) and then thionylchloride (1.16 mL, 16 mmol) were added at room temperature. The mixture was stirred for 30 min and flashed through a short chromatography column (SiO_2, CH_2Cl_2). The solvent was removed under reduced pressure and the product dried in vacuo.

5.1.2.24. Benzo[*b*]furan-2-carbonyl chloride[27] (17). Preparation from benzo[*b*]furan-2-carboxylic acid (Acros) as described above. Yield: 2.16 g (78%) of colorless crystals. Mp 139.4–139.7 °C. IR (KBr): ν (cm^{-1}) = 3128, 1784, 1723.

5.1.2.25. 5-Benzyloxy-benzo[*b*]furan-2-carbonyl chloride (18). Preparation from **16** as described above. Yield: 2.61 g (59%) of colorless crystals. Mp 99.3–102.5 °C. IR (KBr): ν (cm^{-1}) = 2875, 1787, 1730. Anal. ($C_{16}H_{11}ClO_3$): Calcd C, 67.03; H, 3.87. Found: C, 67.74; H, 4.15.

5.1.2.26. Procedure j—Preparation of the N-protected indoles. The protection was performed according to the previously published procedure.[19]

5.1.2.27. 1-Phenylsulfonyl-1*H*-indole[34] (19). From 1*H*-indole (Merck). Yield: 8.20 g (76%).

5.1.2.28. 5-Benzyloxy-1-phenylsulfonyl-1*H*-indole[18] (20). From 5-benzyloxy-1*H*-indole (Lancaster). Yield: 19.72 g. (87%).

5.1.2.29. Procedure k—Preparation of the N-protected benzofuranylindolylmethanones. To a stirred solution of the respective 1-phenylsulfonyl-1*H*-indole **19** or **20** (11.07 mmol) in dry THF (30.0 mL), *n*-butyllithium (7.61 mL 1.6 M in hexane, 12.17 mmol) was added at −78 °C. After 1 h, a pre-cooled solution of the respective benzo[*b*]furan-2-carbonyl chloride **17** or **18** (11.07 mmol) in THF (40.0 mL) was added at once. The mixture was further stirred for 30 min at −78 °C, then allowed to reach room temperature, poured into water (300 mL), and extracted with ethyl acetate (3× 50 mL). The combined organic layers were dried (Na_2SO_4) and the solvent removed under reduced pressure. The crude product was purified by column chromatography (SiO_2, DCM and light petrol 2:1) and subsequent crystallization.

5.1.2.30. (Benzo[*b*]furan-2-yl)-(1-phenylsulfonyl-1*H*-indol-2-yl)-methanone (21). Yield: 1.60 g (33%) of colorless crystals. Mp 144.8–145.5 °C (from methanol). IR (KBr): ν (cm^{-1}) = 3112, 1649. ^1H NMR (DMSO-d_6): δ (ppm) = 7.36–7.46 (m, 2H), 7.53-7.58 (m, 1H), 7.60–7.64 (m, 4H), 7.71–7.82 (m, 3H), 7.89 (d, 1H, J = 7.7 Hz), 7.94 (d, 1H, J = 1.1 Hz), 7.99–8.02 (m, 2H), 8.08 (dd, 1H, J = 8.5 Hz, 0.8 Hz). EI-MS (70 eV) *m*/*z* (%): 401 (82) [M^+], 337 (61), 260 (66), 232 (86), 204 (53), 143 (100), 89 (47), 77 (81). Anal. ($C_{23}H_{15}NO_4S$): Calcd C, 68.81; H, 3.77; N 3.49. Found: C, 68.59; H, 3.60: N, 3.44.

5.1.2.31. (5-Benzyloxybenzo[*b*]furan-2-yl)-(5-benzyloxy-1-phenylsulfonyl-1*H*-indol-2-yl)methanone (22). Yield: 3.80 g (53%) of red crystals. Mp 206.5–206.6 °C (from dichloromethane by addition of diethyl ether). IR (KBr): ν (cm^{-1}) = 1646. ^1H NMR (DMSO-d_6): δ (ppm) = 5.14 (s, 2H), 5.17 (s, 2H), 7.23 (dd, 1H, J = 9.2 Hz, 2.6 Hz), 7.28–7.51 (m, 14H), 7.59–7.64 (m, 2H), 7.70–7.73 (m, 2H), 7.79 (d, 1H, J = 0.8 Hz), 7.92–7.99 (m, 3H). ES-MS (CH_2Cl_2/MeOH, NH_4Ac) *m*/*z* (%): 631 (9) [$M + NH_4^+$], 614 (100) [MH^+]. Anal. ($C_{37}H_{27}NO_6S$): Calcd C, 72.41; H, 4.43; N, 2.28; S, 5.23. Found: C, 71.81; H, 4.43; N, 2.23; S, 5.17.

5.1.2.32. Procedure l—Removal of the phenylsulfonyl protection group. The respective (1-phenylsulfonyl-1*H*-indol-2-yl)benzo[*b*]furan-2-yl-methanone **21** or **22** (1.49 mmol) was suspended in a mixture of THF, MeOH, and an aqueous NaOH (10%) solution (150 mL, 1:1:1). After a 4-h refluxing period, the organic solvents were removed under reduced pressure. The formed precipitate was filtered off, washed with water, dried, and purified by column chromatography (SiO_2, CH_2Cl_2) and subsequent crystallization.

5.1.2.33. (Benzo[*b*]furan-2-yl)-(1*H*-indol-2-yl)methanone (23). Yield: 0.26 g (67%) of yellow crystals. Mp 241.9–242.0 °C (from dichloromethane). IR (KBr): ν (cm^{-1}) = 3293, 1609. ^1H NMR (DMSO-d_6): δ (ppm) = 7.11–7.17 (m, 1H), 7.32–7.44 (m, 2H), 7.51–7.62 (m, 2H), 7.79–7.91 (m, 4H), 8.05 (d, 1H, J = 0.8 Hz), 12.09 (s, 1H, exchangeable). EI-MS (70 eV) *m*/*z* (%): 261 (99) [M^+], 143 (100), 115 (26), 89 (33). Anal. ($C_{17}H_{11}NO_2$): Calcd C, 78.15; H ,4.24; N, 5.36. Found: C, 78.06; H, 4.25; N, 5.32.

5.1.2.34. (5-Benzyloxybenzo[*b*]furan-2-yl)-(5-benzyloxy-1*H*-indol-2-yl)methanone (24). Yield: 0.54 g (76%) of yellow crystals. Mp 183.8–183.9 °C (from dichloromethane). IR (KBr): ν (cm^{-1}) = 3311, 1605. ^1H NMR (DMSO-d_6): δ (ppm) = 5.14 (s, 2H), 5.18 (s, 2H), 7.09 (dd, 1H, J = 8.9 Hz, 2.3 Hz), 7.25–7.52 (m, 14H), 7.71 (d, 1H, J = 1.4 Hz), 7.75 (d, 1H, J = 9.3 Hz), 7.91 (d, 1H, J = 0.8 Hz), 11.96 (d, 1H, J = 1.9 Hz, exchangeable). EI-MS (70 eV) *m*/*z* (%): 473 (20) [M^+], 382 (23), 91 (100). Anal. ($C_{31}H_{23}NO_4$): Calcd C, 78.63; H, 4.90; N, 2.96. Found: C, 78.66; H, 4.99; N, 2.94.

5.1.2.35. Procedure m—Hydrogenolytic preparation of compound 25. A suspension of **23** (0.76 g; 1.60 mmol), ammonium formate (1.01 g; 16.0 mmol), and activated Pd on charcoal (10%, 0.20 g) in a mixture of THF/MeOH (1:1; 300 mL) was heated to reflux for 1 h. The catalyst was filtered over Celite, the solvent removed under reduced pressure, and the product purified by column chromatography (SiO_2, DCM and AcOEt 2:1). Most of the solvent was removed under reduced

pressure and the product crystallized from the solution by addition of light petrol.

5.1.2.36. 5-Hydroxybenzo[*b*]furan-2-yl-(5-hydroxy-1*H*-indol-2-yl)methanone (25). Yield: 0.39 g (83%) of light yellow crystals. Mp 265.3–265.5 °C. IR (KBr): ν (cm^{-1}) = 3453, 3314, 1599. ^1H NMR (DMSO-d_6): δ (ppm) = 6.89 (dd, 1H, J = 8.9 Hz, 2.3 Hz), 7.01–7.04 (m, 2H), 7.12 (d, 1H, J = 2.5 Hz), 7.32 (d, 1H, J = 8.8 Hz), 7.60–7.63 (m, 2H), 7.84 (m, 1H, J = 0.8 Hz), 9.04 (s, 1H, exchangeable), 9.52 (s, 1H, exchangeable), 11.76 (d, 1H, J = 1.1 Hz, exchangeable). EI-MS (70 eV) m/z (%): 293 (68) [M^+], 159 (100). Anal. ($C_{17}H_{11}NO_4$): Calcd C, 69.62; H, 3.78; N, 4.78. Found: C, 69.59; H, 3.97; N, 4.74.

5.2. Biochemical and cellular assays

All activity tests were performed as previously described.[19]

5.3. Molecular modeling

As previously described,[19] an initial computer model of the FLT3 kinase was generated from the PDB crystal structure 1rjb[31] using the molecular modeling package SYBYL 7.1 (Tripos Inc., St. Louis, USA) on a Silicon Graphics Octane workstation. The conformers of compd **7**, *ap*/*ap*, *ap*/*sp*, and *sp*/*sp*, their energies and rotational barriers were calculated by the semi-empirical quantum chemical program AMPAC 8.15 (Semichem Inc., 7128 Summit, Shawnee, KS66216, USA) with the AM1 hamiltonian, the TRUSTE minimization algorithm, and the COSMO water solvation model[35] as implied in SYBYL 7.1. After docking of compd **7**, the FLT3-ligand complexes were energy-minimized using the AMBER 99 force field[36] with AMBER 99 charges for the protein (distance-dependent dielectricity constant 4, first 50 cycles with constrained backbone and the steepest descent method). For that purpose, compound **7** was provided with AMBER 99 atom types by analogy with corresponding amino acid atoms, as well as with Gasteiger–Hueckel charges. New parameters describing the central OC(CH)COC(CH)O moiety had to be added to the AMBER 99 force field (derived from the Tripos force field and from comparison with similar AMBER parameters). The final minimization up to a RMS gradient of 0.05 kcal/(mol Å) was performed with the Powell conjugate gradient method. Considerations on the PDGFR kinase were based on the FLT3 crystal structure with simple mutation of the only different binding site residue, FLT3 Phe-691, into PDGFR Thr-681.

References and notes

1. Pietras, K.; Sjoblom, T.; Rubin, K.; Heldin, C. H.; Ostman, A. *Cancer Cell* **2003**, *3*, 439–443.
2. Parcells, B. W.; Ikeda, A. K.; Simms-Waldrip, T.; Moore, T. B.; Sakamoto, K. M. *Stem Cells* **2006**, *24*, 1174–1184.
3. Scheijen, B.; Griffin, J. D. *Oncogene* **2002**, *21*, 3314–3333.
4. Board, R.; Jayson, G. C. *Drug Resist. Updat.* **2005**, *8*, 75–83.
5. Morgan, M. A.; Reuter, C. W. *Ann. Hematol.* **2006**, *85*, 139–163.
6. Schmidt-Arras, D.; Schwable, J.; Böhmer, F. D.; Serve, H. *Curr. Pharm. Des.* **2004**, *10*, 1867–1883.
7. Tickenbrock, L.; Müller-Tidow, C.; Berdel, W. E.; Serve, H. *Expert Opin. Emerg. Drugs* **2006**, *11*, 153–165.
8. Gazit, A.; Yee, K.; Uecker, A.; Böhmer, F. D.; Sjoblom, T.; Ostman, A.; Waltenberger, J.; Golomb, G.; Banai, S.; Heinrich, M. C.; Levitzki, A. *Bioorg. Med. Chem.* **2003**, *11*, 2007–2018.
9. Pandey, A.; Volkots, D. L.; Seroogy, J. M.; Rose, J. W.; Yu, J. C.; Lambing, J. L.; Hutchaleelaha, A.; Hollenbach, S. J.; Abe, K.; Giese, N. A.; Scarborough, R. M. *J. Med. Chem.* **2002**, *45*, 3772–3793.
10. Stone, R. M.; DeAngelo, D. J.; Klimek, V.; Galinsky, I.; Estey, E.; Nimer, S. D.; Grandin, W.; Lebwohl, D.; Wang, Y.; Cohen, P.; Fox, E. A.; Neuberg, D.; Clark, J.; Gilliland, D. G.; Griffin, J. D. *Blood* **2005**, *105*, 54–60.
11. Mesters, R. M.; Padro, T.; Bieker, R.; Steins, M.; Kreuter, M.; Goner, M.; Kelsey, S.; Scigalla, P.; Fiedler, W.; Buchner, T.; Berdel, W. E. *Blood* **2001**, *98*, 241–243.
12. Fiedler, W.; Serve, H.; Dohner, H.; Schwittay, M.; Ottmann, O. G.; O'Farrell, A. M.; Bello, C. L.; Allred, R.; Manning, W. C.; Cherrington, J. M.; Louie, S. G.; Hong, W.; Brega, N. M.; Massimini, G.; Scigalla, P.; Berdel, W. E.; Hossfeld, D. K. *Blood* **2005**, *105*, 986–993.
13. Wilhelm, S. M.; Carter, C.; Tang, L.; Wilkie, D.; McNabola, A.; Rong, H.; Chen, C.; Zhang, X.; Vincent, P.; McHugh, M.; Cao, Y.; Shujath, J.; Gawlak, S.; Eveleigh, D.; Rowley, B.; Liu, L.; Adnane, L.; Lynch, M.; Auclair, D.; Taylor, I.; Gedrich, R.; Voznesensky, A.; Riedl, B.; Post, L. E.; Bollag, G.; Trail, P. A. *Cancer Res.* **2004**, *64*, 7099–7109.
14. Smith, B. D.; Levis, M.; Beran, M.; Giles, F.; Kantarjian, H.; Berg, K.; Murphy, K. M.; Dauses, T.; Allebach, J.; Small, D. *Blood* **2004**, *103*, 3669–3676.
15. Lopes de Menezes, D. E.; Peng, J.; Garrett, E. N.; Louie, S. G.; Lee, S. H.; Wiesmann, M.; Tang, Y.; Shephard, L.; Goldbeck, C.; Oei, Y.; Ye, H.; Aukerman, S. L.; Heise, C. *Clin. Cancer Res.* **2005**, *11*, 5281–5291.
16. Sattler, M.; Verma, S.; Byrne, C. H.; Shrikhande, G.; Winkler, T.; Algate, P. A.; Rohrschneider, L. R.; Griffin, J. D. *Mol. Cell. Biol.* **1999**, *19*, 7473–7480.
17. Böhmer, F. D.; Karagyozov, L.; Uecker, A.; Serve, H.; Botzki, A.; Mahboobi, S.; Dove, S. *J. Biol. Chem.* **2003**, *278*, 5148–5155.
18. Mahboobi, S.; Teller, S.; Pongratz, H.; Hufsky, H.; Sellmer, A.; Botzki, A.; Uecker, A.; Beckers, T.; Baasner, S.; Schächtele, C.; Überall, F.; Kassack, M. U.; Dove, S.; Böhmer, F. D. *J. Med. Chem.* **2002**, *45*, 1002–1018.
19. Mahboobi, S.; Uecker, A.; Sellmer, A.; Cénac, C.; Höcher, H.; Pongratz, H.; Eichhorn, E.; Hufsky, H.; Trümpler, A.; Sicker, M.; Heidel, F.; Fischer, T.; Stocking, C.; Elz, S.; Böhmer, F. D.; Dove, S. *J. Med. Chem.* **2006**, *49*, 3101–3115.
20. Royer, R.; Guillaumel, J. *J. Heterocycl. Chem.* **1986**, *23*, 1277–1282.
21. Nagahara, M.; Nakanishi, T.; Kuriyama, K.; Ikemoto, M.; Yamamoto, M. (Kaken Pharma Co. Ltd.) *Jpn. Kokai Tokkyo Koho* **1984**, JP59231080.
22. Nagahara, M.; Kuriyama, K.; Ikemoto, M.; Nakanishi, T. *Yakugaku Zasshi* **1985**, *105*, 840–844.
23. Nagahara, M.; Oishi, Y.; Takehisa, Y.; Yajima, M.; Kurokawa, S.; Kajikawa, N. (Kaken Pharma Co. Ltd.) *Jpn. Kokai Tokkyo Koho* **1985**, JP60181081.
24. Nagahara, M.; Kuriyama, K.; Hiyama, Y.; Ito, K.; Ikemoto, M.; Nakanishi, T. *Yakugaku Zasshi* **1986**, *106*, 27–35.
25. Kondo, A. (Sharp Kk.) *Jpn. Kokai Tokkyo Koho* **1996**, JP8295688.

26. Mahboobi, S.; Pongratz, H.; Hufsky, H.; Hockemeyer, J.; Frieser, M.; Lyssenko, A.; Paper, D. H.; Bürgermeister, J.; Böhmer, F. D.; Fiebig, H. H.; Burger, A. M.; Baasner, S.; Beckers, T. *J. Med. Chem.* **2001**, *44*, 4535–4553.
27. Reichstein, T.; Ignaz, R. *Helv. Chim. Acta* **1930**, *13*, 1275–1281.
28. Reichstein, T.; Oppenauer, R.; Grussner, A.; Hirt, R.; Rhyner, L.; Glatthaar, C. *Helv. Chim. Acta* **1935**, *18*, 816–830.
29. Schmeck, C.; Müller, U.; Schmidt, G.; Pernerstorfer, J.; Bischoff, H.; Kretschmer, A.; Vöhringer, V.; Faeste, C.; Haning, H.; Hauswald, M.; Schmidt, D.; Zoche, M.; Apeler, H.; Jonghaus, W.; Reinemer, P. (Bayer AG) *Ger. Offen.* **2002**, DE10115408.
30. Lu, J.; Ma, T.; Nagpal, S.; Shen, Q.; Warshawsky, A. M.; Ochoada, J. M.; Yee, Y. K. (Eli Lilly & Co.) *PCT Int. Appl.* **2005**, WO2005051938.
31. Griffith, J.; Black, J.; Faerman, C.; Swenson, L.; Wynn, M.; Lu, F.; Lippke, J.; Saxena, K. *Mol. Cell* **2004**, *13*, 169–178.
32. Mohammadi, M.; Froum, S.; Hamby, J. M.; Schroeder, M. C.; Panek, R. L.; Lu, G. H.; Eliseenkova, A. V.; Green, D.; Schlessinger, J.; Hubbard, S. R. *EMBO J.* **1998**, *17*, 5896–5904.
33. Zahao, D. J.; Huang, J. K.; Shan, Z. X. *Chin. Chem. Lett.* **1993**, *99*, 385–386.
34. Sundberg, R. J.; Russel, F. *J. Org. Chem.* **1973**, *38*, 3324–3330.
35. Klamt, A. *J. Phys. Chem.* **1995**, *99*, 2224–2235.
36. Cornell, W. D.; Cieplak, P.; Bayly, C. I.; Gould, I. R.; Merz, K. M. J.; Ferguson, D. M.; Spellmeyer, D. C.; Fox, T.; Caldwell, J. W.; Kollman, P. A. *J. Am. Chem. Soc.* **1995**, *117*, 5179–5197.